

Auto-Oxidation of a Volatile Silicon Compound: A Theoretical Study of the Atmospheric Chemistry of Tetramethylsilane

Zhonghua Ren, Gabriel da Silva*

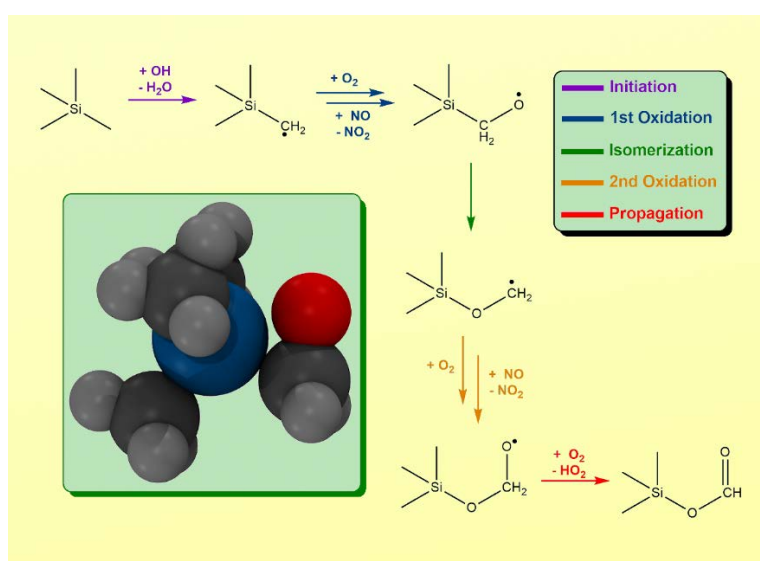
Department of Chemical Engineering, The University of Melbourne, Parkville 3010, Australia.

*E-mail: gdasilva@unimelb.edu.au. Phone: +61 3 8344 6627.

ABSTRACT

Volatile silicon compounds (VOSiCs) are air pollutants present in both indoor and outdoor environments. Here, tetramethylsilane (TMS) is selected as a model to study the photochemical oxidation mechanisms for VOSiCs using *ab initio* and RRKM theory / master equation kinetic modelling. Under tropospheric conditions the TMS radical $(\text{CH}_3)_3\text{SiCH}_2^\bullet$ reacts with O_2 to produce a stabilized peroxy radical which is expected to ultimately yield the alkoxy radical $(\text{CH}_3)_3\text{SiCH}_2\text{O}^\bullet$. At combustion-relevant temperatures, however, a well-skiping reaction to $(\text{CH}_3)_3\text{SiO}^\bullet + \text{HCHO}$ dominates. Importantly, the $(\text{CH}_3)_3\text{SiCH}_2\text{O}^\bullet$ radical is predicted to rearrange to $(\text{CH}_3)_3\text{SiOCH}_2^\bullet$ with a very low reaction barrier, enabling an auto-oxidation process involving addition of a second O_2 . Subsequent oxidation reaction mechanisms of $(\text{CH}_3)_3\text{SiOCH}_2^\bullet$ have been developed, with the major product predicted to be the ester $(\text{CH}_3)_3\text{SiOCHO}$, an experimentally observed TMS oxidation product. The production of substantially oxygenated compounds following a single radical initiation reaction has implications for the ability of VOSiCs to contribute to ozone and particle formation in both outdoor and indoor environments.

TOC Graphic



KEYWORDS: Tetramethylsilane, photochemical oxidation, mechanism, kinetics, ester

Introduction

Volatile silicon compounds (VOSiCs) are present in a wide range of household items, particularly in personal care products such as cosmetics and deodorants.¹⁻⁴ Of particular interest are the cyclic polysiloxanes, such as hexamethylcyclotrisiloxane (D3), octamethylcyclotetrasiloxane (D4) and decamethylcyclopentasiloxane (D5) which are emerging persistent chemicals of concern.⁵⁻¹⁰ Volatile siloxanes have been detected at significant concentrations in both indoor and outdoor environments.¹¹ For example, it was recently shown that D4 was the most abundant volatile compound in a university classroom.¹² In urban outdoor air silicon compounds can also be found at high levels.¹³⁻¹⁴

Despite their significance, the atmospheric chemistry of silicon compounds remains relatively unstudied. Importantly, we do not know if the Si heteroatom alters the classical reaction processes expected for oxygenated hydrocarbons. So as to begin exploring these processes, here we have chosen to study the atmospheric chemistry of tetramethylsilane (TMS), $\text{Si}(\text{CH}_3)_4$, one of the simplest VOSiCs. TMS is also an important volatile compound in its own right, as an emerging solvent and industrial chemical.¹⁵⁻¹⁶ Its high temperature oxidation chemistry is also of interest as it is a precursor for the flame synthesis of silicon nanoparticles¹⁷ and Si coatings via chemical vapor deposition in semiconductor manufacturing.¹⁸⁻¹⁹ Previous studies have established that the first stage of TMS oxidation involves H abstraction (*e.g.* by $\cdot\text{OH}$) to form the $(\text{CH}_3)_3\text{SiCH}_2\cdot$ radical,²⁰⁻²⁶ although further reactions of this species have not been well studied.

In this paper, theoretical simulations – both quantum chemical and statistical reaction rate theory modelling – have been used to study the oxidation of the TMS radical $(\text{CH}_3)_3\text{SiCH}_2\cdot$. This work reveals that a single radical initiator can result in an auto-oxidation cascade, in which two O_2 molecules are added to ultimately form the oxygenated species $(\text{CH}_3)_3\text{SiOHCO}$. The understanding of silicon oxidation chemistry gained from this study will help in the development of photochemical oxidation mechanisms for larger (and more computationally demanding) structures.

Methods

The G4²⁷ model chemistry is used to explore the TMS oxidation mechanism, using the Gaussian 16²⁸ program. G4 is a composite method which is expected to predict reaction barriers with mean uncertainty of less than 1 kcal mol⁻¹.²⁹ All geometries are optimized at the B3LYP/6-31g(2df,p) level of theory, with these structures then used to calculate electronic energies using HF and post-SCF calculations up to CCSD(T), combined with empirical corrections. All reported transition states have one imaginary frequency, with connectivity to both reactants and products confirmed by intrinsic reaction coordinate calculations.

Kinetics calculations have been conducted to obtain reaction rates, yields and branching ratios using the MultiWell 2017 program suite,³⁰ based on the G4 model chemistry results. Reaction pathways with no barriers are treated by the restricted Gorin Model.³¹ Capture rates for the reactions $(\text{CH}_3)_3\text{SiCH}_2\cdot + \text{O}_2$ and $(\text{CH}_3)_3\text{Si}\cdot + \text{HCHO}$ are calculated as 1.21×10^{-11} and 1.02×10^{-10} cm³ molecule⁻¹ s⁻¹, respectively, using long-range transition state theory.³²⁻³³ Calculation of microcanonical rate coefficients uses RRKM theory with internal degrees of freedom treated as harmonic oscillators and external degrees of freedom approximated as a symmetric top comprising an active 1D K-rotor and inactive 2D J-rotor in

the sums and densities of states. In MultiWell's hybrid master equation, the energy grained component consisted of 2000 grains of 10 cm^{-1} , with the continuum component then extended up to $150,000 \text{ cm}^{-1}$. Each simulation comprised 10^7 trials with sufficient collisions to reach steady-state.

Results and Discussion

It is understood that TMS oxidation will be initiated in the atmosphere via reaction with $\cdot\text{OH}$ (and to a lesser extent other radical species), producing the alkyl radical $(\text{CH}_3)_3\text{SiCH}_2\cdot$. The TMS + $\cdot\text{OH}$ rate coefficient is measured to be around $1 \times 10^{-12} \text{ cm}^3 \text{ molecule}^{-1} \text{ s}^{-1}$,²⁴⁻²⁶ corresponding to a TMS lifetime of about 10 days in the troposphere. Subsequently, $(\text{CH}_3)_3\text{SiCH}_2\cdot$ will associate with O_2 to produce the peroxy radical $(\text{CH}_3)_3\text{SiCH}_2\text{O}_2\cdot$. It has been proposed²³ that unimolecular isomerization of $(\text{CH}_3)_3\text{SiCH}_2\text{O}_2\cdot$ to $(\text{CH}_3)_3\text{SiOCH}_2\text{O}\cdot$ is responsible for the photochemical oxidation of TMS to the ester $(\text{CH}_3)_3\text{SiOCHO}$, which we now consider.

A potential energy surface for reaction of the $(\text{CH}_3)_3\text{SiCH}_2\cdot$ radical with O_2 is shown in Figure 1. The process begins with O_2 addition to the alkyl radical site to form the peroxy radical $(\text{CH}_3)_3\text{SiCH}_2\text{O}_2\cdot$ (**1**); this is a barrierless and significantly exothermic step ($-28.9 \text{ kcal mol}^{-1}$). Figure 1 shows three subsequent unimolecular reaction channels that have been identified. First, $(\text{CH}_3)_3\text{SiCH}_2\text{O}_2\cdot$ can shift a H atom from its methylene group via **TS1** ($11.7 \text{ kcal mol}^{-1}$ above reactants) with a barrier of $40.6 \text{ kcal mol}^{-1}$. Alternatively, a H atom shift from the methyl group gives the hydroperoxyalkyl radical **3**, $(\text{CH}_3)_2\text{Si}(\text{CH}_2\text{O}_2\text{H})\text{CH}_2\cdot$ ($11.0 \text{ kcal mol}^{-1}$ below the entrance channel) via **TS2** which sits $24.8 \text{ kcal mol}^{-1}$ above $(\text{CH}_3)_3\text{SiCH}_2\text{O}_2\cdot$ and $4.1 \text{ kcal mol}^{-1}$ below the reactants. From here, $(\text{CH}_3)_2\text{Si}(\text{CH}_2\text{O}_2\text{H})\text{CH}_2\cdot$ can eliminate $\cdot\text{OH}$ to form a cyclic species $c\text{-(CH}_3)_2\text{SiCH}_2\text{OCH}_2\cdot$ + $\cdot\text{OH}$ via **TS3** with a barrier of $20.7 \text{ kcal mol}^{-1}$. Based on the relatively high reaction barriers, the first two reaction pathways are unlikely to contribute under atmospheric conditions. The third pathway, which has the lowest energy barrier, involves isomerization of the peroxy radical via **TS4** (22 kcal mol^{-1} above **1** and $6.9 \text{ kcal mol}^{-1}$ below the reactants). As predicted by Atkinson et al.²³ this reaction proceeds via attack of the radical site at the Si atom. However, this mechanism passes through the unstable $(\text{CH}_3)_3\text{SiOOCH}_2\cdot$ structure to form a weakly-bound postreaction adduct (**4**), in a very exothermic process, which subsequently decomposes to $(\text{CH}_3)_3\text{SiO}\cdot$ + HCHO. Importantly, this mechanism does not proceed via $(\text{CH}_3)_3\text{SiOCH}_2\text{O}\cdot$, and therefore does not provide an explanation for ester formation in silane oxidation.

With the excess energy from association of $(\text{CH}_3)_3\text{SiCH}_2\cdot$ and O_2 , chemically activated $(\text{CH}_3)_3\text{SiCH}_2\text{O}_2\cdot$ can potentially undergo direct well-skipping dissociation to $(\text{CH}_3)_3\text{SiO}\cdot$ + HCHO. This process, however, is in competition with both collisional quenching of the peroxy radical and reverse dissociation to the reactants. To better understand this process, RRKM theory-based master equation simulations have been used to study the kinetics from 300 to 1500 K at 1 atm N_2 . Calculated product yields are shown in Figure 2, with rate coefficients plotted in Figure 3 (data listed as Supporting Information). According to Figure 1, over 98 % of $(\text{CH}_3)_3\text{SiCH}_2\text{O}_2\cdot$ is deactivated via N_2 collisions at 300 K, with the remainder of the activated population predicted to undergo reverse reaction to $(\text{CH}_3)_3\text{SiCH}_2\cdot$. Despite having a negative barrier relative to this back reaction, dissociation to $(\text{CH}_3)_3\text{SiO}\cdot$ + HCHO is predicted to be insignificant at 300 K, which can be attributed to the tight nature of the transition state and its commensurately low entropy. As temperature increases from 300 to 1500 K, the stabilized yield of $(\text{CH}_3)_3\text{SiCH}_2\text{O}_2\cdot$ decreases dramatically, at the expense of the back-reaction channel. Figure 3 demonstrates that this appears as significant fall-off in the total predicted (phenomenological) rate

coefficient as temperature increases. There is also, however, an increase in the dissociation channel to $(\text{CH}_3)_3\text{SiO}^\bullet + \text{HCHO}$ as temperature increases (see Figure 2 inset), which overtakes the RO_2 stabilization channel at temperatures of around 800 K and above. Accordingly, the direct reaction $(\text{CH}_3)_3\text{SiCH}_2^\bullet + \text{O}_2 \rightarrow (\text{CH}_3)_3\text{SiO}^\bullet + \text{HCHO}$ is predicted to be important in the thermal oxidation chemistry of TMS, but will be insignificant under tropospheric conditions.

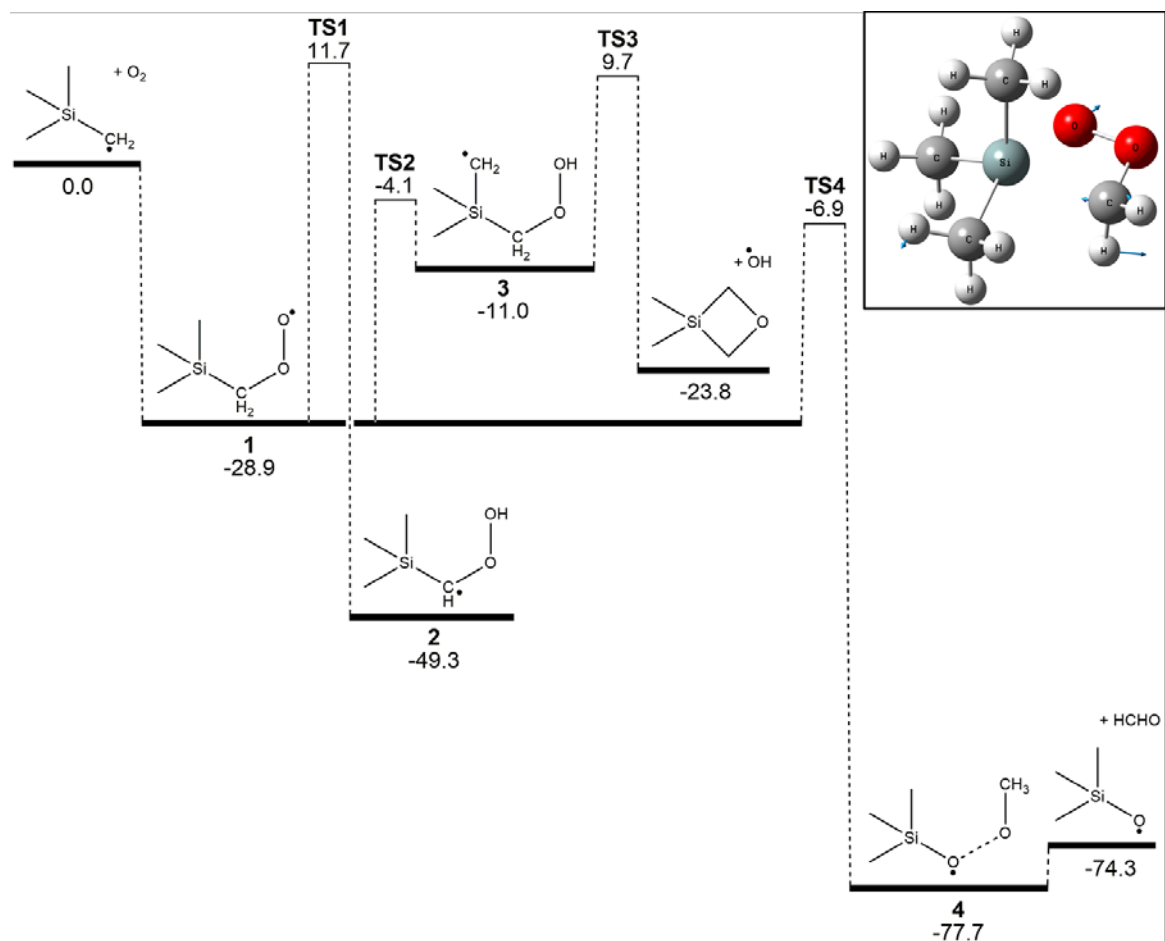


Figure 1. Potential energy surface for the $(\text{CH}_3)_3\text{SiCH}_2^\bullet + \text{O}_2$ reaction. Energies calculated at the G4 level of theory (0 K enthalpies) in units of kcal mol^{-1} . Inset shows the structure of key transition state **TS4** and its imaginary frequency displacement vectors.

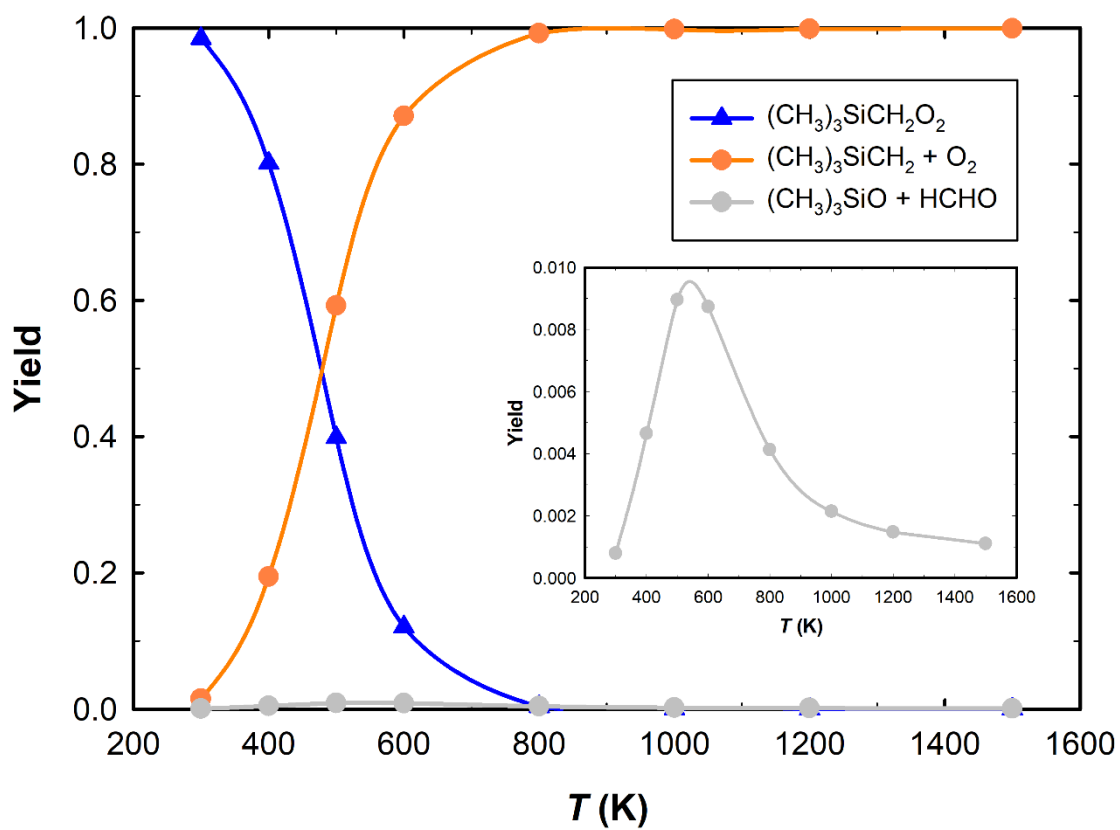


Figure 2. Calculated yields for the $(\text{CH}_3)_3\text{SiCH}_2^* + \text{O}_2$ reaction from master equation simulations at 300 to 1500 K and 1 atm N_2 .

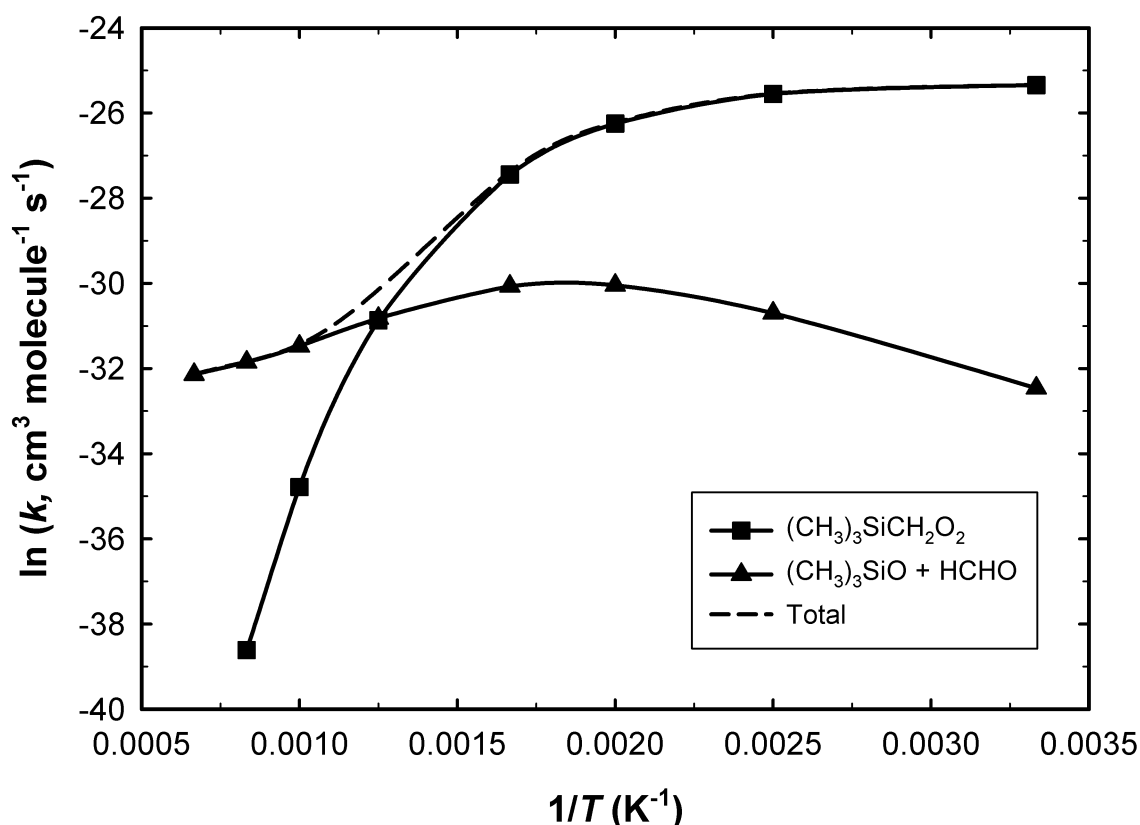


Figure 3. Calculated rate coefficients k for the $(\text{CH}_3)_3\text{SiCH}_2^* + \text{O}_2$ reaction from master equation simulations at 300 to 1500 K and 1 atm N_2 .

The peroxy radical $(\text{CH}_3)_3\text{SiCH}_2\text{O}_2^*$ is expected as a primary atmospheric oxidation product of TMS, which will subsequently be converted to the alkoxy radical $(\text{CH}_3)_3\text{SiCH}_2\text{O}^*$ (**5**) via reaction with NO and other radicals. We have therefore studied the subsequent reactions of $(\text{CH}_3)_3\text{SiCH}_2\text{O}^*$. Bimolecular H abstraction from $(\text{CH}_3)_3\text{SiCH}_2\text{O}^*$ by O_2 , forming $(\text{CH}_3)_3\text{SiCHO}$, proceeds with a significant barrier of 12.9 kcal mol⁻¹ (see Supporting Information), and is expected to be relatively slow. Unimolecular reaction chemistry will therefore dominate.

A potential energy surface for unimolecular reaction of $(\text{CH}_3)_3\text{SiCH}_2\text{O}^*$ is shown in Figure 4. This alkoxy radical can eliminate HC^*O via **TS5** to yield $(\text{CH}_3)_3\text{SiH}$, with a barrier of 28.3 kcal mol⁻¹. Conventional β -scission can also take place, via a barrierless pathway, producing $(\text{CH}_3)_3\text{Si}^* + \text{HCHO}$ with a thermodynamic barrier of 17.7 kcal mol⁻¹. Isomerization of $(\text{CH}_3)_3\text{SiCH}_2\text{O}^*$ begins with concerted Si—C bond breaking and Si—O bond formation via **TS6**, which sits only 2.8 kcal mol⁻¹ above the alkoxy radical. This reaction is exothermic by 26.2 kcal mol⁻¹ and produces the alkyl radical $(\text{CH}_3)_3\text{SiOCH}_2^*$ (**6**). This unique rearrangement is not available to the corresponding structures without silicon, and may therefore significantly alter the photochemical oxidation mechanisms of volatile silicon compounds in comparison to their conventional oxygenated hydrocarbon analogues. Following oxidation to $(\text{CH}_3)_3\text{SiOCH}_2^*$, an internal 1,4 H-shift from a methyl group to the radical site can proceed via **TS7** (25.5 kcal mol⁻¹ above $(\text{CH}_3)_3\text{SiOCH}_2^*$ and 0.7 kcal mol⁻¹ below $(\text{CH}_3)_3\text{SiCH}_2\text{O}^*$), yielding the alkyl radical

$(\text{CH}_3)_2\text{Si}(\text{OCH}_3)\text{CH}_2^\bullet$ (**7**) which sits 22.1 kcal mol⁻¹ below the alkoxy radical $(\text{CH}_3)_3\text{SiCH}_2\text{O}^\bullet$. Considering the energy barriers and well depths, isomerization of **5** to **6** and **7** is expected to be rapid, even at room temperature. Note that this will take place through both chemically activated and thermal reaction mechanisms; the $(\text{CH}_3)_3\text{SiCH}_2\text{O}_2^\bullet + \text{NO} \rightarrow (\text{CH}_3)_3\text{SiCH}_2\text{O}_2 + \text{NO}_2$ reaction is exothermic by 20.5 kcal mol⁻¹, at the G4 level of theory, and this energy will be substantially distributed between the vibrational modes of the reaction products (as well as to inactive translational and rotational degrees of freedom), enhancing reaction rates over those at thermally equilibrated conditions.

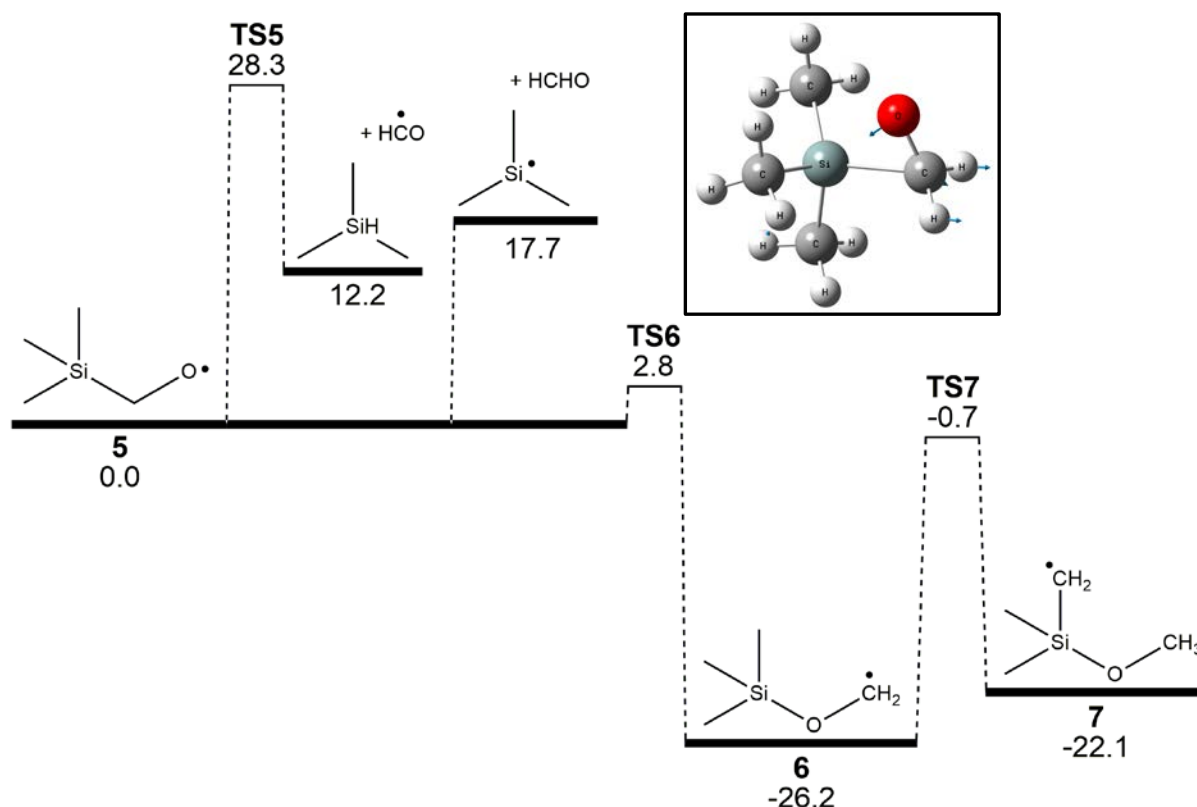


Figure 4. Potential energy surface for $(\text{CH}_3)_3\text{SiCH}_2\text{O}^\bullet$ decomposition and isomerization. Energies calculated at the G4 level of theory (0 K enthalpies) in units of kcal mol⁻¹. Inset shows the structure of key transition state **TS6** and its imaginary frequency displacement vectors.

To better understand the unimolecular reaction kinetics of $(\text{CH}_3)_3\text{SiCH}_2\text{O}^\bullet$ we carried out master equation simulations at 1 atm N₂ for temperatures between 300 and 1500 K, and at 300 K with initial vibrational energies offset in excess of the Maxwell Boltzmann distribution ($E_{\text{offset}} = 0 - 20$ kcal mol⁻¹). The results are summarized in Figure 5. All simulations were run for sufficient time to achieve complete loss of the starting reactant, and therefore the non-zero offset calculations incorporate both the chemical and thermal activation processes.³⁴ Even at the slowest reaction conditions of 300 K, loss of the alkoxy radical is rapid, with 99 % of the initial population disappearing within 20 nanoseconds. The bimolecular reaction of $(\text{CH}_3)_3\text{SiCH}_2\text{O}^\bullet$ with O₂ will be uncompetitive in comparison.

Figure 5 reveals that at 300 K the $(\text{CH}_3)_3\text{SiCH}_2\text{O}^\bullet$ radical isomerizes exclusively to $(\text{CH}_3)_3\text{SiOCH}_2^\bullet$. As temperature / internal energy increases the isomerization to $(\text{CH}_3)_2\text{Si}(\text{OCH}_3)\text{CH}_2^\bullet$ becomes significant, with a predicted yield of *ca.* 5 % at 500 K / 7 % at 15 kcal mol⁻¹ offset. Only at more energetic conditions does dissociation to $(\text{CH}_3)_3\text{SiO}^\bullet + \text{HCHO}$ become important, and this is not predicted to be an important atmospheric process. Under tropospheric conditions, given mild chemical activation of the $(\text{CH}_3)_3\text{SiCH}_2\text{O}^\bullet$ radical, we propose that stabilized $(\text{CH}_3)_3\text{SiOCH}_2^\bullet$ will be the major product, with some minor formation of $(\text{CH}_3)_2\text{Si}(\text{OCH}_3)\text{CH}_2^\bullet$. Importantly, both species are carbon-centred alkyl radicals, and are thus able to associate with O₂. This unique alkoxy radical mechanism available to silanes therefore enables auto-oxidation chemistry, in which a single radical initiator (*e.g.* $\bullet\text{OH}$) makes a free radical which undergoes a near-instantaneous cascade of chemical reactions, with the possibility for molecular weight growth and the production of highly oxygenated products.

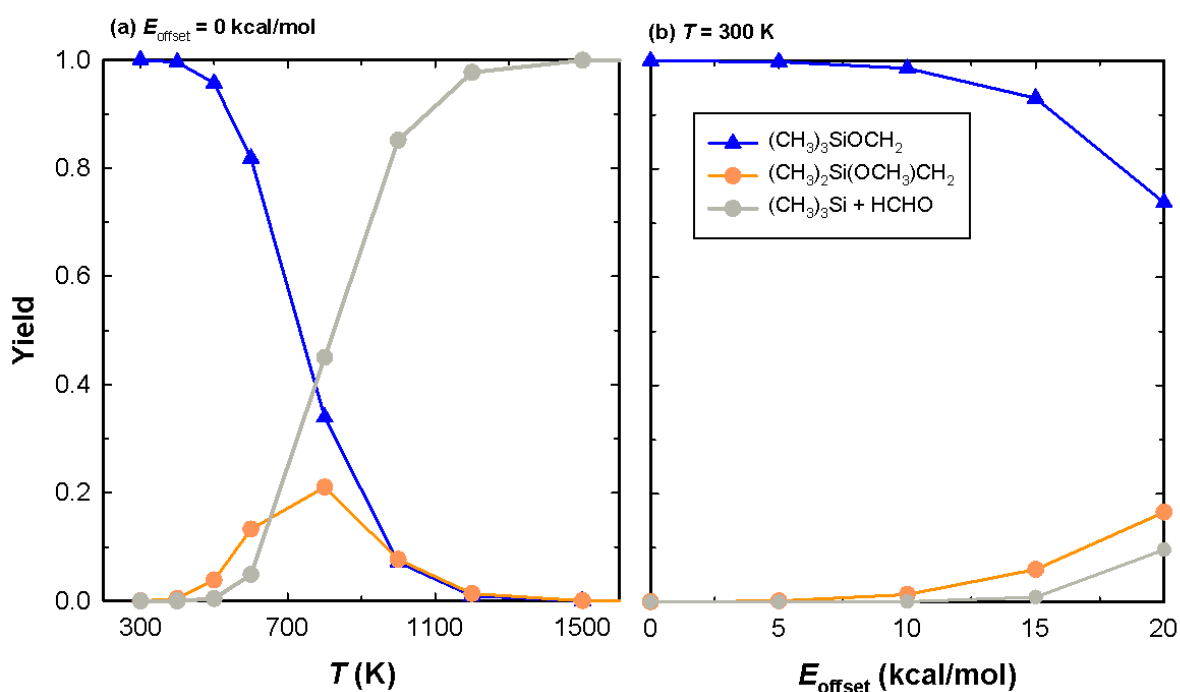


Figure 5. Calculated yields for the unimolecular isomerization and decomposition of $(\text{CH}_3)_3\text{SiCH}_2\text{O}^\bullet$ from master equation simulations at (a) $T = 300$ to 1500 K with $E_{\text{offset}} = 0$ kcal mol⁻¹, and (b) $E_{\text{offset}} = 0$ to 20 kcal mol⁻¹ with $T = 300$ K.

Figure 6 depicts subsequent oxidation mechanisms of $(\text{CH}_3)_3\text{SiOCH}_2^\bullet$ (**6**) by O₂. Similar to the $(\text{CH}_3)_3\text{SiCH}_2^\bullet + \text{O}_2$ reaction, it is initiated by barrierless O₂ addition at the radical centre, forming the peroxy radical $(\text{CH}_3)_3\text{SiOCH}_2\text{O}_2^\bullet$ (**8**) with 35.7 kcal mol⁻¹ exothermicity. The peroxy radical $(\text{CH}_3)_3\text{SiOCH}_2\text{O}_2^\bullet$ can undergo a facile intramolecular H shift from methyl group to produce the radical $(\text{CH}_3)_2\text{Si}(\text{OCH}_2\text{O}_2\text{H})\text{CH}_2^\bullet$ (**9**) via **TS8** (20.3 kcal mol⁻¹ above $(\text{CH}_3)_3\text{SiOCH}_2\text{O}_2^\bullet$ and 15.4 kcal mol⁻¹ below the reactants). From here, two different decomposition pathways have been identified. $(\text{CH}_3)_2\text{Si}(\text{OCH}_2\text{O}_2\text{H})\text{CH}_2^\bullet$ can eliminate OH \bullet via radical attack at a peroxide O atom, yielding the five-membered ring structure **10** via **TS9**, which is 21.5 kcal mol⁻¹ above $(\text{CH}_3)_2\text{Si}(\text{OCH}_2\text{O}_2\text{H})\text{CH}_2^\bullet$ and 2.0

kcal mol⁻¹ below the reactants. Competing with this pathway, a 1,4-H shift from the methylene moiety in (CH₃)₂Si(OCH₂O₂H)CH₂[•] can occur via **TS10**, at 3.3 kcal mol⁻¹ below the reactants (1.3 kcal mol⁻¹ below **TS9**). Ultimately, this again releases [•]OH, along with (CH₃)₃SiOCHO (**12**). Although these unimolecular reaction mechanisms may contribute to the high temperature oxidation of (CH₃)₃SiOCH₂[•], the relatively high barriers for decomposition and deep well depth for peroxy radical formation mean that it will undergo conventional collisional deactivation in the atmosphere.

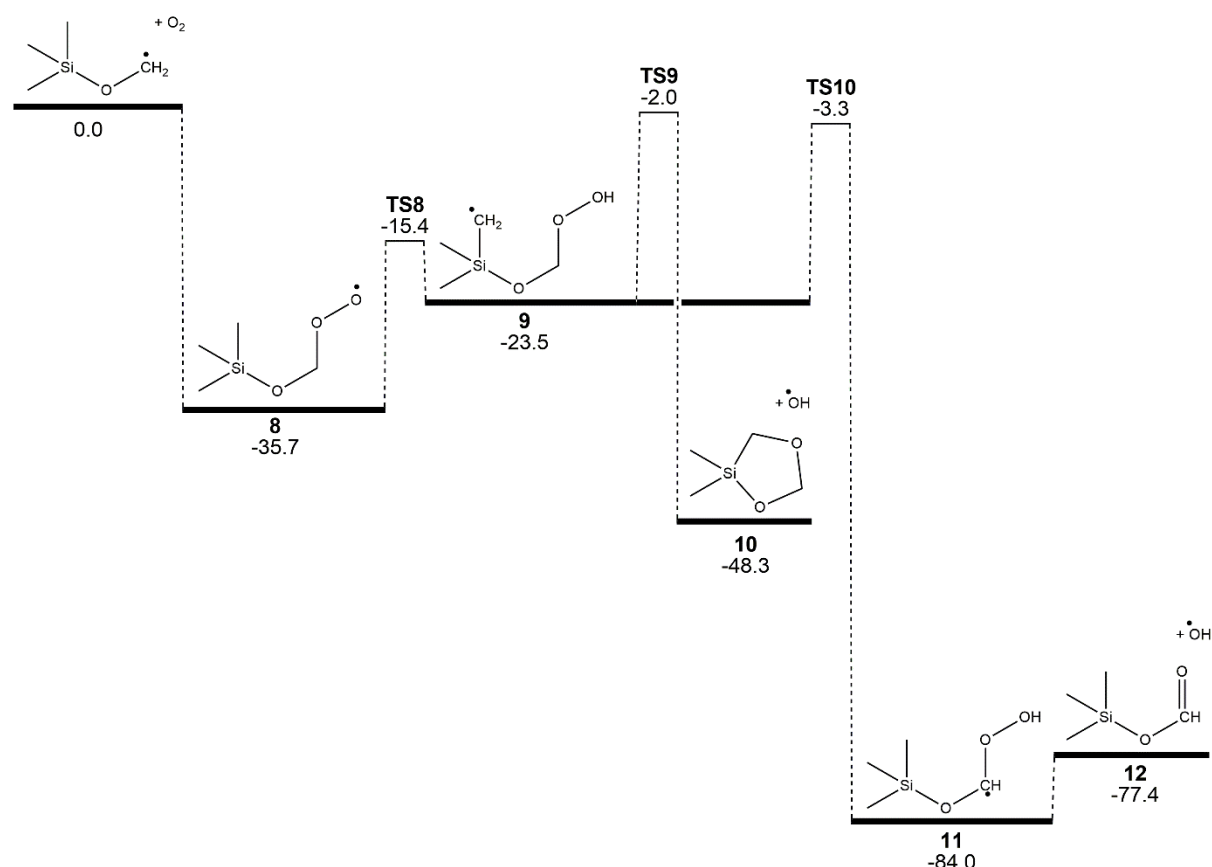


Figure 6. Potential energy surface for the (CH₃)₃SiOCH₂[•] + O₂ reaction. Energies calculated at the G4 level of theory (0 K enthalpies) in units of kcal mol⁻¹.

In the atmospheric oxidation of TMS, the (CH₃)₃SiOCH₂[•] + O₂ reaction will ultimately produce the alkoxy radical (CH₃)₃SiOCH₂O[•] (**13**), *e.g.*, via RO₂ + NO chemistry. A potential energy surface for further unimolecular reaction of (CH₃)₃SiOCH₂O[•] is shown in Figure 7. In competition, H abstraction to O₂ may also take place, with a predicted barrier height of 4.7 kcal mol⁻¹, forming the ester (CH₃)₃SiOCHO (**12**) (see Supporting Information). According to Figure 7 we see that the dominant fragmentation reaction of (CH₃)₃SiOCH₂O[•] is also likely to be to (CH₃)₃SiOCHO (+ H[•]), where the barrier height is 15.1 kcal mol⁻¹ (**TS13**). Alternatively, decomposition can occur via O–C bond breaking according to transition state **TS12** with a barrier of 30.5 kcal mol⁻¹, fragmenting to (CH₃)₃SiO[•] + HCHO. Finally, (CH₃)₃SiOCH₂O[•] can also isomerize through H abstraction from a methyl group, with a 15.3 kcal mol⁻¹ barrier (**TS14**), leading to the alkyl radical (CH₃)₂Si(OCH₂OH)CH₂[•] (**14**) which sits 3.2 kcal mol⁻¹ below (CH₃)₃SiOCH₂O[•]. Subsequently, (CH₃)₂Si(OCH₂OH)CH₂[•] can undergo a second intramolecular H abstraction, from the

methylene group, via **TS15** with a barrier of 19.2 kcal mol⁻¹ (16.0 kcal mol⁻¹ relative to the reactant), producing (CH₃)₃SiOC[•]HOH (**15**).

Given the relatively high barriers for decomposition of (CH₃)₃SiOCH₂O[•], its dominant atmospheric fate is likely to be reaction with O₂, although decomposition is expected to ultimately form the same products, in (CH₃)₃SiOCHO + HO₂[•]. The ester (CH₃)₃SiOCHO has been observed experimentally as the major oxidation product of TMS.²³ Although this prior study proposed that isomerization of (CH₃)₃SiCH₂O₂[•] was the source of (CH₃)₃SiOCH₂O[•] and thus (CH₃)₃SiOCHO, we find that it actually arises from a similar isomerization reaction in the (CH₃)₃SiCH₂O[•] alkoxy radical.

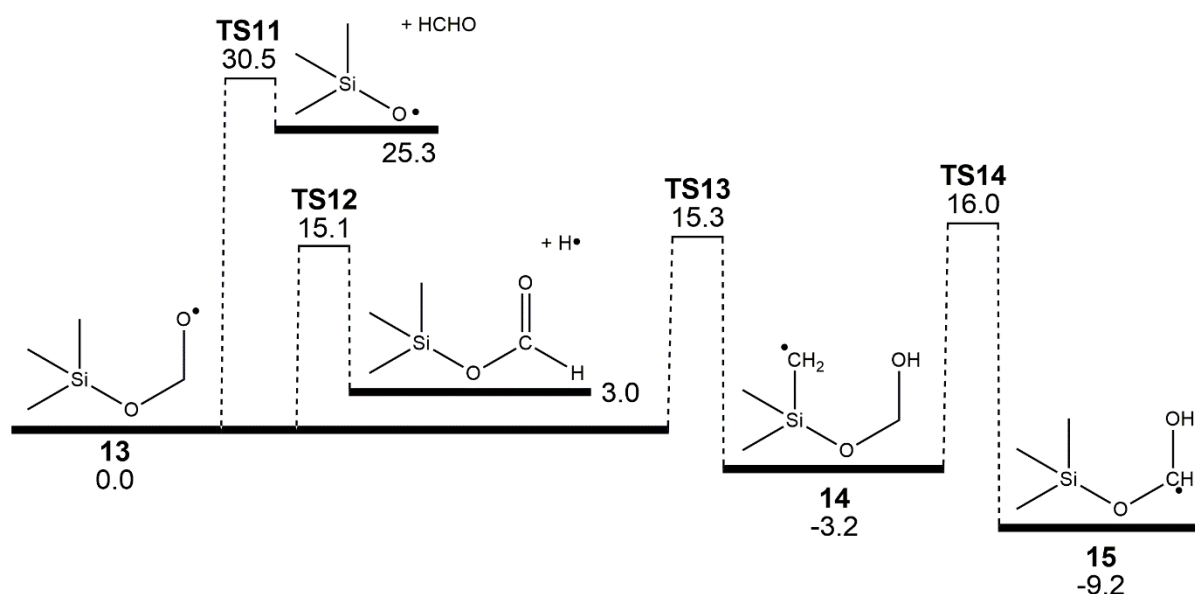
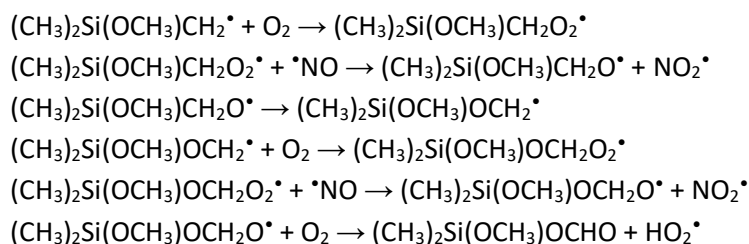
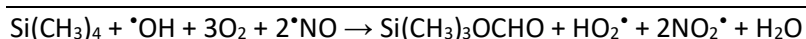
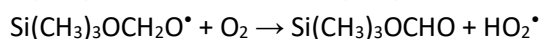
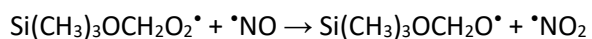
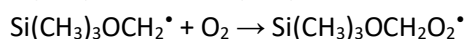
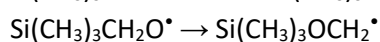
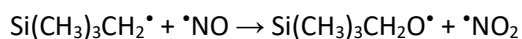
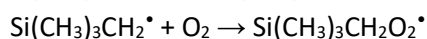
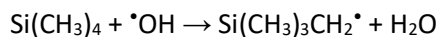


Figure 7. Potential energy surface for (CH₃)₃SiOCH₂O[•] isomerization and decomposition. Energies calculated at the G4 level of theory (0 K enthalpies) in units of kcal mol⁻¹.

Given that (CH₃)₂Si(OCH₃)CH₂[•] is expected as a minor TMS oxidation product, its further reactions are due some consideration. Again, this alkyl radical will associate with O₂, leading to an intermediate alkoxy radical that can undergo a further isomerization (with 2.0 kcal mol⁻¹ barrier height, see Supporting Information). A second auto-oxidation step is then available, yielding (CH₃)₂Si(OCH₃)OCHO as the stable end product. The proposed reaction sequence is:



In conclusion, this work has identified that auto-oxidation facilitated by alkoxy radical isomerization controls the photochemical oxidation of tetramethylsilane, one of the simplest volatile silicon compounds. The major steps in this reaction scheme are summarized in Figure 8 and listed below:



We find that the net result of this reaction mechanism is the conversion of TMS into the ester $\text{Si}(\text{CH}_3)_3\text{OCHO}$, along with propagation of the single initiating $\cdot\text{OH}$ radical to $\text{HO}_2\cdot$ and the conversion of two NO radicals to NO_2 . The formation of $\text{Si}(\text{CH}_3)_3\text{OCHO}$ is significant in that it does not result in fragmentation of TMS, retaining all five heavy atoms, along with the introduction of two oxygens. This will result in a substantial decrease in volatility, with increased likelihood to partition to the particle phase, resulting from a single radical initiator. The conversion of multiple NO radicals to NO_2 is also significant, as their subsequent photolysis will ultimately create two ozone molecules.

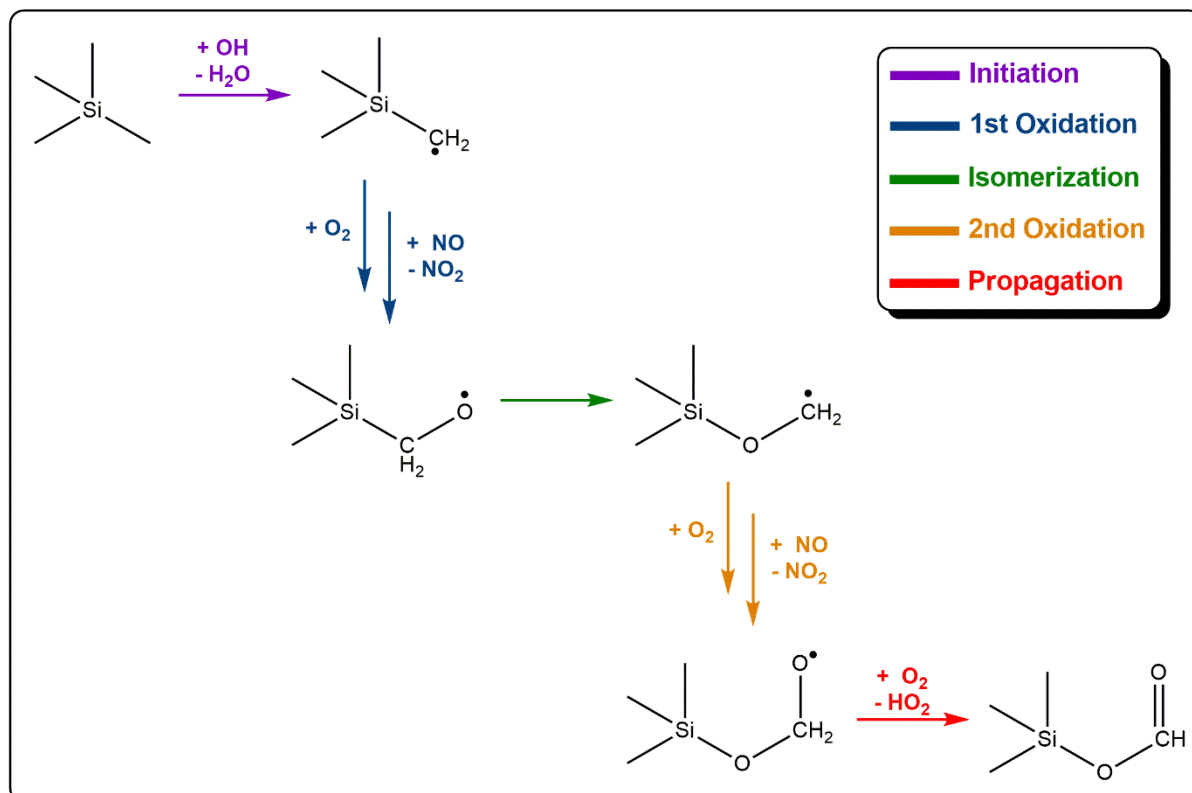


Figure 8. Proposed reaction scheme for the OH radical initiated auto-oxidation of tetramethylsilane.

Summary and Conclusions

This work studied the atmospheric degradation of the tetramethylsilane radical $(\text{CH}_3)_3\text{SiCH}_2^\bullet$ using computational chemistry modelling and master equation simulations. Reaction with O_2 leads to the peroxy radical $(\text{CH}_3)_3\text{SiCH}_2\text{O}_2^\bullet$, which in turn makes the alkoxy radical $(\text{CH}_3)_3\text{SiCH}_2\text{O}^\bullet$. A novel isomerization process is revealed for this alkoxy radical, which forms the alkyl radical $(\text{CH}_3)_3\text{SiOCH}_2^\bullet$. This enables a second oxidation step, eventually forming the ester $(\text{CH}_3)_3\text{SiOCHO}$, an experimentally observed product of tetramethylsilane oxidation. The overall effect of this auto-oxidation scheme is to convert tetramethylsilane to a highly oxygenated product following a single radical initiation event, which also coincides with the conversion of two NO radicals to ozone-promoting NO_2 .

Supporting Information Available: Calculated rate coefficients for the $(\text{CH}_3)_3\text{SiCH}_2^\bullet + \text{O}_2$ reaction, potential energy surfaces for the $(\text{CH}_3)_3\text{SiCH}_2\text{O}^\bullet + \text{O}_2$ reaction, $(\text{CH}_3)_3\text{SiOCH}_2\text{O}^\bullet + \text{O}_2$ reaction and $(\text{CH}_3)_2\text{Si}(\text{OCH}_3)\text{CH}_2\text{O}^\bullet$ isomerisation, and coordinates for wells and products.

Acknowledgements

This work was supported in part by the Australian Research Council Future Fellowship scheme. We are grateful to Christa Fittschen for helpful discussions.

References

1. Dudzina, T.; von Goetz, N.; Bogdal, C.; Biesterbos, J. W.; Hungerbühler, K., Concentrations of cyclic volatile methylsiloxanes in European cosmetics and personal care products: Prerequisite for human and environmental exposure assessment. *Environment International* **2014**, *62*, 86-94.
2. Capela, D.; Alves, A.; Homem, V.; Santos, L., From the shop to the drain—Volatile methylsiloxanes in cosmetics and personal care products. *Environment International* **2016**, *92-93*, 50-62.
3. Chandra, G., *Organosilicon materials*. Springer: 1997; Vol. 3; pp 16-23.
4. McDonald, B. C.; de Gouw, J. A.; Gilman, J. B.; Jathar, S. H.; Akherati, A.; Cappa, C. D.; Jimenez, J. L.; Lee-Taylor, J.; Hayes, P. L.; McKeen, S. A., Volatile chemical products emerging as largest petrochemical source of urban organic emissions. *Science* **2018**, *359* (6377), 760-764.
5. Rücker, C.; Kümmerer, K., Environmental chemistry of organosiloxanes. *Chemical Reviews* **2015**, *115* (1), 466-524.
6. Bernard, F.; Papanastasiou, D. K.; Papadimitriou, V. C.; Burkholder, J. B., Temperature dependent rate coefficients for the gas-phase reaction of the OH radical with linear (L₂, L₃) and cyclic (D₃, D₄) permethylsiloxanes. *The Journal of Physical Chemistry A* **2018**, *122* (17), 4252-4264.
7. Coggon, M. M.; McDonald, B. C.; Vlasenko, A.; Veres, P. R.; Bernard, F.; Koss, A. R.; Yuan, B.; Gilman, J. B.; Peischl, J.; Aikin, K. C., Diurnal variability and emission pattern of decamethylcyclopentasiloxane (D5) from the application of personal care products in two North American cities. *Environmental Science & Technology* **2018**, *52* (10), 5610-5618.
8. Chandramouli, B.; Kamens, R. M., The photochemical formation and gas–particle partitioning of oxidation products of decamethyl cyclopentasiloxane and decamethyl tetrasiloxane in the atmosphere. *Atmospheric Environment* **2001**, *35* (1), 87-95.
9. Mackay, D.; Cowan-Ellsberry, C. E.; Powell, D. E.; Woodburn, K. B.; Xu, S.; Kozerski, G. E.; Kim, J., Decamethylcyclopentasiloxane (D5) environmental sources, fate, transport, and routes of exposure. *Environmental Toxicology and Chemistry* **2015**, *34* (12), 2689-2702.
10. Janecek, N. J.; Hansen, K. M.; Stanier, C. O., Comprehensive atmospheric modeling of reactive cyclic siloxanes and their oxidation products. *Atmospheric Chemistry and Physics* **2017**, *17* (13), 8357-8370.
11. Wang, D.-G.; Norwood, W.; Alaei, M.; Byer, J. D.; Brimble, S., Review of recent advances in research on the toxicity, detection, occurrence and fate of cyclic volatile methyl siloxanes in the environment. *Chemosphere* **2013**, *93* (5), 711-725.
12. Tang, X.; Misztal, P. K.; Nazaroff, W. W.; Goldstein, A. H., Siloxanes are the most abundant volatile organic compound emitted from engineering students in a classroom. *Environmental Science & Technology Letters* **2015**, *2* (11), 303-307.
13. Genualdi, S.; Harner, T.; Cheng, Y.; MacLeod, M.; Hansen, K. M.; van Egmond, R.; Shoeib, M.; Lee, S. C., Global distribution of linear and cyclic volatile methyl siloxanes in air. *Environmental Science & Technology* **2011**, *45* (8), 3349-3354.
14. Tran, T. M.; Le, H. T.; Vu, N. D.; Dang, G. H. M.; Minh, T. B.; Kannan, K., Cyclic and linear siloxanes in indoor air from several northern cities in Vietnam: levels, spatial distribution and human exposure. *Chemosphere* **2017**, *184*, 1117-1124.
15. Ab Rani, M. A.; Borduas, N.; Colquhoun, V.; Hanley, R.; Johnson, H.; Larger, S.; Lickiss, P. D.; Llopis-Mestre, V.; Luu, S.; Mogstad, M., The potential of methylsiloxanes as solvents for synthetic chemistry applications. *Green Chemistry* **2014**, *16* (3), 1282-1296.
16. Graiver, D.; Farminer, K. W.; Narayan, R., A review of the fate and effects of silicones in the environment. *Journal of Polymers and the Environment* **2003**, *11* (4), 129-136.

17. Janzen, C.; Knipping, J.; Rellinghaus, B.; Roth, P., Formation of silica-embedded iron-oxide nanoparticles in low-pressure flames. *Journal of Nanoparticle Research* **2003**, *5* (5-6), 589-596.
18. Rynders, S. W.; Scheeline, A.; Bohn, P. W., Structure evolution in α -SiC:H films prepared from tetramethylsilane. *Journal of Applied Physics* **1991**, *69* (5), 2951-2960.
19. Lee, M.-S.; Bent, S. F., Spectroscopic and thermal studies of α -SiC:H film growth: Comparison of mono-, tri-, and tetramethylsilane. *Journal of Vacuum Science & Technology A* **1998**, *16* (3), 1658-1663.
20. Oueslati, I.; Kerkeni, B.; Spielfiedel, A.; Tchang-Brillet, W.-Ü. L.; Feautrier, N., Ab initio investigation of the abstraction reactions by H and D from tetramethylsilane and its deuterated substitutions. *The Journal of Physical Chemistry A* **2014**, *118* (5), 791-802.
21. Zhang, H.; Zhang, G.-l.; Liu, J.-y.; Hou, W.-j.; Liu, B.; Li, Z.-s., Dual-level direct dynamics studies on the reactions of tetramethylsilane with chlorine and bromine atoms. *Theoretical Chemistry Accounts* **2010**, *125* (1), 75.
22. Lazarou, Y. G.; Papagiannakopoulos, P., Kinetic studies of the reaction of chlorine atoms with tetramethylsilane. *The Journal of Physical Chemistry* **1993**, *97* (26), 6806-6810.
23. Atkinson, R.; Tuazon, E. C.; Kwok, E. S. C.; Arey, J.; Aschmann, S. M.; Bridier, I., Kinetics and products of the gas-phase reactions of $(\text{CH}_3)_4\text{Si}$, $(\text{CH}_3)_3\text{SiCH}_2\text{OH}$, $(\text{CH}_3)_3\text{SiOSi}(\text{CH}_3)_3$ and $(\text{CD}_3)_3\text{SiOSi}(\text{CD}_3)_3$ with Cl atoms and OH radicals. *Journal of the Chemical Society, Faraday Transactions* **1995**, *91* (18), 3033-3039.
24. Tuazon, E. C.; Aschmann, S. M.; Atkinson, R., Atmospheric degradation of volatile methyl-silicon compounds. *Environmental Science & Technology* **2000**, *34* (10), 1970-1976.
25. Sommerlade, R.; Parlar, H.; Wrobel, D.; Kochs, P., Product analysis and kinetics of the gas-phase reactions of selected organosilicon compounds with OH radicals using a smog chamber-mass spectrometer system. *Environmental Science & Technology* **1993**, *27* (12), 2435-2440.
26. Atkinson, R., Kinetics of the gas-phase reactions of a series of organosilicon compounds with OH and NO_3 radicals and O_3 at 297 ± 2 K. *Environmental Science & Technology* **1991**, *25* (5), 863-866.
27. Curtiss, L. A.; Redfern, P. C.; Raghavachari, K., Gaussian-4 theory. *The Journal of Chemical Physics* **2007**, *126* (8), 084108.
28. Frisch, M.; Trucks, G.; Schlegel, H.; Scuseria, G.; Robb, M.; Cheeseman, J.; Scalmani, G.; Barone, V.; Petersson, G.; Nakatsuji, H., Gaussian 16, revision A 2016.
29. Zheng, J.; Zhao, Y.; Truhlar, D. G., The DBH24/08 database and its use to assess electronic structure model chemistries for chemical reaction barrier heights. *Journal of Chemical Theory and Computation* **2009**, *5* (4), 808-821.
30. Barker, J. R.; Nguyen, T. L.; Stanton, J. F.; Aieta, C.; Ceotto, M.; Gabas, F.; Kumar, T. J. D.; Li, C. G. L.; Lohr, L. L.; Maranzana, A., MultiWell-2017 Software Suite; University of Michigan. *Ann Arbor, Michigan, USA, Jan* **2017**.
31. Smith, G. P.; Golden, D. M., Application of RRKM theory to the reactions $\text{OH} + \text{NO}_2 + \text{N}_2 \rightarrow \text{HONO}_2 + \text{N}_2$ (1) and $\text{ClO} + \text{NO}_2 + \text{N}_2 \rightarrow \text{ClONO}_2 + \text{N}_2$ (2); A modified gorin model transition state. *International Journal of Chemical Kinetics* **1978**, *10* (5), 489-501.
32. Georgievskii, Y.; Klippenstein, S. J., Long-range transition state theory. *The Journal of Chemical Physics* **2005**, *122* (19), 194103.
33. Greenwald, E. E.; North, S. W.; Georgievskii, Y.; Klippenstein, S. J., A two transition state model for radical-molecule reactions: A case study of the addition of OH to C_2H_4 . *The Journal of Physical Chemistry A* **2005**, *109* (27), 6031-6044.
34. Pinches, S. J.; da Silva, G., On the separation of timescales in chemically activated reactions. *International Journal of Chemical Kinetics* **2013**, *45* (6), 387-396.